Microchemical Journal 186 (2023) 108323

Contents lists available at ScienceDirect

Microchemical Journal

journal homepage: www.elsevier.com/locate/microc

Review Article

How to dissect viral infections and their interplay with the host-proteome by immunoaffinity and mass spectrometry: A tutorial

Hugo M. Santos [a,b,*], Luís B. Carvalho [a,b], Carlos Lodeiro [a,b], Gonçalo Martins [a,b], Inês L. Gomes [c], Wilson D.T. Antunes [c], Vanessa Correia [d], Maria M. Almeida-Santos [e], Helena Rebelo-de-Andrade [d,f], António P.A. Matos [g], J.L. Capelo [a,b,*]

[a] BIOSCOPE Research Group, LAQV-REQUIMTE, Department of Chemistry, NOVA School of Science and Technology, Universidade NOVA de Lisboa, 2829-516 Caparica, Portugal
[b] PROTEOMASS Scientific Society, Madan Parque, Rua dos Inventores, 2825-182 Caparica, Portugal
[c] Instituto Universitário Militar, Centro de Investigação da Academia Militar (CINAMIL), Unidade Militar Laboratorial de Defesa Biológica e Química (UMLDBQ), Av. Dr. Alfredo Bensaúde, 1849-012 Lisbon, Portugal
[d] Antiviral Resistance Lab, Research & Development Unit, Infectious Diseases Department, Instituto Nacional de Saúde Doutor Ricardo Jorge, IP, Av. Padre Cruz, 1649-016 Lisbon, Portugal
[e] Clinical Pathology Laboratory, Hospital Curry Cabral, EPE, Centro Hospitalar de Lisboa Central, EPE, Rua da Beneficência, nº8, 1069-166 Lisbon, Portugal
[f] Host-Pathogen Interaction Unit, Research Institute for Medicines (iMed.ULisboa), Faculty of Pharmacy, Universidade de Lisboa, Av. Professor Gama Pinto, 1649-003 Lisboa, Portugal
[g] Centro de Investigação Interdisciplinar Egas Moniz (CiiEM), Cooperativa de Ensino Superior Egas Moniz, Quinta da Granja, 2829-511 Caparica, Portugal

ARTICLE INFO

Keywords:
Immuno-mass spectrometry
Viral detection
MALDI-TOF-MS
LC-ESI-Q-TOF-MS/MS

ABSTRACT

The capabilities of bioanalytical mass spectrometry to (i) detect and differentiate viruses at the peptide level whilst maintaining high sample throughput and (ii) to provide diagnosis and prognosis for infected patients are presented as a tutorial in this work to aid analytical chemists and physicians to gain insights into the possibilities offered by current high-resolution mass spectrometry technology and bioinformatics. From (i) sampling to sample treatment; (ii) Matrix-Assisted Laser Desorption Ionization- to Electrospray Ionization -based mass spectrometry; and (iii) from clustering to peptide sequencing; a detailed step-by-step guide is provided and exemplified using SARS-CoV-2 Spike Y839 variant and the variant of concern SARS-CoV-2 Alpha (B.1.1.7 lineage), Influenza B, and Influenza A subtypes AH1N1pdm09 and AH3N2.

1. Introduction

The coronavirus disease 2019 (COVID-19) has resulted in almost 540 million reported cases and more than 6,3 million deaths worldwide as of June 2022 [1]. The causative infectious agent of this disease is the severe acute respiratory syndrome coronavirus 2 (SARS-CoV-2) [2–5].

This virus belongs to the Coronaviridae family and the Betacoronavirus genus. SARS-CoV-2 diagnosis is a challenge in continuous updating. Two main ways of detecting the virus are currently applied. One relies on the reverse transcription-polymerase chain reaction (RT-PCR), and the other one on immunoassays. Protocols devoted to using these methods have been created in a few months during 2020 and are applied by personnel lacking training in analytical chemistry. The World Health Organization (WHO) has advised that many COVID-19-positive cases are false because PCRs are being run using several cycles too high. For the case of many commercial immunoassays, especially those adapted in point-of-care devices, sensitivity and selectivity have not been validated by independent agencies. Furthermore, it is unclear how current immunoassays respond to another coronavirus other than SARS-CoV-2. Moreover, mutations are an additional challenge as mutated viruses might not be detected with current specific immunoassays and PCRs. Also, there are additional limits to RT-PCR analysis, such as the detergents used to deactivate the virus, which can inhibit PCR reaction [6], the heating to denature the virus, which can affect the detection in specimens with low viral load, resulting in false negatives [7], or the false positives arising from unintended amplification of contaminants.

Mass spectrometry has long been used to uncover the structure and

* Corresponding authors at: BIOSCOPE Research Group, Department of Chemistry, NOVA School of Science and Technology, Universidade NOVA de Lisboa, 2829-516 Caparica, Portugal.
E-mail addresses: hmsantos@fct.unl.pt (H.M. Santos), jlcm@fct.unl.pt (J.L. Capelo).

https://doi.org/10.1016/j.microc.2022.108323
Received 27 September 2022; Received in revised form 11 December 2022; Accepted 13 December 2022
Available online 16 December 2022

Nomenclature

AmBic	Ammonium bicarbonate
ACN	Acetonitrile
Covid-19	Coronavirus disease 2019
DTT	1,4-Dithio-DL-threitol
E	Envelope
EM	Electronic Microscopy
ESI	Electrospray Ionization
FA	Formic acid
FASP	Filter-Aided Sample Preparation
HPLC	High-Performance Liquid Chromatography
IAA	Iodoacetamide
IP	Immunoaffinity Purification
LC	Liquid Chromatography
M	Membrane
MALDI-TOF-MS	Matrix-Assisted Laser Desorption Ionization Time-of-Flight Mass Spectrometry
MS	Mass Spectrometry
MWCO	Molecular Weight Cut-Off
N	Nucleocapsid
PBS	Phosphate-Buffered Saline
Q	Quadrupole
RNA	Ribonucleic acid
RT	Room Temperature
RT-PCR	Reverse Transcription-Polymerase Chain Reaction
S	Spike
SARS-CoV-2	Severe Acute Respiratory Syndrome Coronavirus 2
SDS	Sodium Dodecyl Sulphate
TEM	Transmission Electron Microscopy
TFA	Trifluoroacetic
TOF	Time of Flight
UA	Ultrasonic Amplitude
UF	Ultrasonic Frequency
UHR	Ultra-High Resolution
US	Ultrasonic
UT	Ultrasonic Time
VTM	Viral Transport Media
WHO	World Health Organization

properties of viruses [8–11]. Recent technological developments have offered improvements in sensitivity, resolution, mass accuracy and bioinformatics, allowing for the analysis of whole viruses and their interactions with the host. Thus, the viruses can be detected using mass spectrometry with the aid of adequate sampling in a wide number of human samples, such as saliva, urine, faeces, blood, sputum, and mucus, or in environmental samples such as food and wastewater. It is worth noting that recovered patients that tested negative for SARS-CoV-2 for RT-PCR analyses tested positive via ESI-based mass spectrometry using parallel reaction monitoring [12].

Focusing on the proteome of SARS-CoV-2, a total of 29 proteins are known, including 4 structural proteins – the Envelope (E), Membrane (M), Nucleocapsid (N) and Spike (S) proteins, and 25 nonstructural proteins [1,2]. The S protein is an interesting target because the S gene is highly divergent between coronaviruses [3]. Because the number of released SARS-COV-2 sequences has increased dramatically under the Global Initiative on Sharing All Influenza Data (GISAID), a specific database of SARS-COV-2 peptides can be built to be used in conjunction with mass spectrometry via Matrix-Assisted Laser Desorption Ionization, MALDI-TOF-MS, and / or electrospray ionisation, ESI, for the rapid identification of SARS-CoV-2 variants in human, animal, and environmental samples. However, despite its great potential, mass spectrometry has not yet received the attention it deserves from the virology and medical communities.

It is our understanding that mass spectrometry shall play a pivotal role in monitoring COVID-19 and future pandemics caused by viruses because it addresses high throughput and specificity and can distinguish strains of the same family based on peptide sequencing. Moreover, the viral load profile of SARS-CoV-2 comprises high levels at around the time of symptom onset [13–18], which potentially renders easier the detection of the virus in human samples. In addition, the problem of collecting low viral loads can be overcome via fast preconcentration techniques after nasopharyngeal swabs sampling of SARS-CoV-2 [18,19]. Furthermore, the use of analytical proteomics can provide medical information for clinical decisions via interpretation of the patient's proteome present in the clinical specimens used to detect the virus.

In this work, we first present immunoaffinity Matrix Assisted Laser Desorption Ionization Time-of-Flight Mass Spectrometry as a fast way to diagnose the disease and immunoaffinity nanoliquid chromatography nano electrospray ionisation quadrupole time of flight mass spectrometry / mass spectrometry, nanoLC-ESI-Q-TOF-MS/MS, as the perfect way to retrieve medical information from the virus-patient interaction. Moreover, we present two different robust sample treatments, the first one to be used as a fast way to obtain the virus-host interactome whilst the second one is an elegant manner of using immunoaffinity and magnetic beads to distinguish SARS-CoV-2 from other respiratory viruses (influenza) rapidly and efficiently. Virus data presented herein is validated against PCR, whilst transmission electronic microscopy (TEM) is used as an orthogonal validation tool. In summary, we present an overview on how-to-use analytical chemistry and bioinformatics to dissect virus infections.

2. Material and methods

2.1. Reagents

All reagents used were mass spectrometry grade, MS grade, or electrophoresis grade. Human monoclonal [CR3022] to SARS-CoV-2 Spike Glycoprotein S1 and Protein A Magnetic Beads were purchased from Abcam (Amsterdam, Netherlands). Iodoacetamide (IAA), urea, phosphate-buffered saline (PBS), formic acid (FA), tris base and Bradford reagent were purchased from Sigma-Aldrich (Basel, Switzerland). Ammonium bicarbonate (AmBic) and hydrochloric acid solution 37 % (HCl) were purchased from Fluka (Basel, Switzerland). Sodium dodecyl sulphate (SDS), acetonitrile (ACN) and boric acid were purchased from Panreac (Barcelona, Spain). 1,4-Dithio-DL-threitol (DTT) was purchased from Alfa Aesar (Haverhill, Massachusetts, USA). Pierce™ trypsin protease MS grade, trifluoroacetic acid (TFA) were purchased from Thermo Fisher Scientific (Waltham, Massachusetts, USA).

2.2. Apparatus

The membrane vivacon 500 10,000 MWCO Hydrosart from Sartorius (Goettingen, Germany) and prism™ refrigerated microcentrifuge from Labnet (New Jersey, USA) were used in the standard Filter Assisted Sample preparation, FASP, and ultrasound FASP methodology. An ultrasonic probe, model UP 50H (dr. Hielscher), was used for protein pellet resuspension. Microplate Horn Assembly equipped with a water recirculation system and operating with the Q700 system (20 kHz) from QSonica (Newtown, CT, USA) was used to accelerate the steps of reduction alkylation and digestion in the ultrasound FASP. A vacuum concentrator centrifuge model UNIVAPO 150 ECH Speed Vac and a vacuum pump model UNIJET II (Munich, Germany) were used for

sample drying. Vortex models ELMI CM70M-09 from SkyLine (Southern California, USA) and VX-200 Vortex Mixer from Labnet (New Jersey, USA) were used in the sample mix. CLARIOstar® High-Performance Monochromator Multimode from BMG LABTECH (Germany) was used for Bradford and total peptide assays. Mass spectrometry data were acquired using a MALDI-TOF-MS Microflex LRF and an ultra-high resolution, UHR-Q-TOF IMPACT HD from Bruker Daltonics (Bremen, Germany). Chromatographic separation of peptides was carried out using an Ultimate 3000 nLC nano-system equipped with a µPAC™ trapping column (PharmaFluidics) and a 50 cm analytical column µPACTM (PharmaFluidics).

2.3. Sample Collection, Processing, and storage

SARS-CoV-2 Spike Y839 variant and Alpha (B.1.1.7 lineage) clinical specimens were collected at Hospital das *Forças Armadas* and then processed in *Laboratório de Bromatologia e Defesa Biológica (Unidade Militar Laboratorial de Defesa Biológica e Química)*. Nasopharyngeal (NP) swab samples were collected and placed in a 3 mL Universal Viral Transport Media (VTM) system. Tubes containing clinical specimens were decontaminated with an alcohol-based solution and identified. After collection, samples were processed immediately. Samples were inactivated by incubation at 95 °C for 10 min and kept at −20 °C until further processing.

Influenza-positive clinical specimens representative of the different types and subtypes causing seasonal epidemics - AH1N1pdm09, AH3N2 and B, were collected at the Hospital Curry Cabral, EPE, *Centro Hospitalar de Lisboa Central*, EPE, Lisbon, Portugal. Combined NP and oropharyngeal (OP) swab specimens were collected from patients hospitalised or followed in ambulatory care during the 2017–2018 influenza season, placed in Universal VTM and kept at −20 °C until further processing. Heat inactivation was used for SARS-CoV-2.

2.4. SARS-CoV-2 immunoaffinity extraction for TEM

Aliquots (30 µL) containing 20, 200 and 2000 plaque-forming units (pfus) of SARS-CoV-2 (BetaCoV/Portugal/ICV1006/2020) were diluted to a final volume of 400 µL with PBS. Then 5 µL of 100 µg/mL Human monoclonal anti-SARS-CoV-2 S Glycoprotein S1 antibody [CR3022] were added, followed by a 20 min incubation at 37 °C with gentle agitation. Afterwards, 70 µL of Protein A Magnetic Beads (ab214286) were added, followed by 20 min incubation at RT with gentle agitation. The samples were placed in a magnetic separator, and the supernatant was withdrawn. The magnetic beads were further washed 5 times with 1 mL of PBS.

Finally, the sample was divided into two tubes for RT-qPCR and transmission electron microscopy (TEM).

2.5. RNA extraction and RT-PCR

Total RNA was extracted from the Immunoaffinity extracted virions using an automated magnetic bead-based nucleic acid purification workstation BioSprint 96 (Qiagen, Hilden, Germany), according to the manufacturer's instructions. Three genes of SARS-CoV-2 (ORF1ab, N, and E) were detected by RT-qPCR using a commercial kit (Fosun 2019-nCoV qPCR) and a BioRad CFX96 qPCR thermal cycler.

2.6. TEM

Magnetic bead suspensions with attached virus particles prepared according to the procedure described in 2.4 were adsorbed onto formvar-carbon coated transmission electron microscope copper grids and stained for 1 min with 2 % aqueous uranyl acetate. COVID-infected Vero Cells used for virus propagation were examined by thin-section electron microscopy using a standard protocol. In brief, cells were fixed in 3 % glutaraldehyde in 0.1 M sodium cacodylate buffer pH 7.3 for 2 h. Following primary fixation, cells were pelleted and embedded in 2 % agar for further processing. Samples were further sequentially fixed in 1 % osmium tetroxide in 0.1 M sodium cacodylate buffer pH 7.3 for 1 h and 1 % uranyl acetate for 1 h. Dehydration was carried out in ethanol. After 2 passages in propylene oxide, samples were embedded in an Epon-Araldite mixture. Thin sections stained with 2 % aqueous uranyl acetate and Reynold's lead citrate were analysed for the presence of virus particles. All the samples were studied and photographed in a JEOL 1200-EX electron microscope.

2.7. qRT-PCR

SARS-CoV-2 ORF1ab, S and *N*-genes and internal control (RNase P) were amplified by qRT-PCR using the TaqMan 2019-nCoV Assay Kit v1 (Thermo Fisher) with TaqMan Fast Virus 1-step Master Mix (Thermo Fisher) and the CFX96 thermocycler (BioRad), according to the following protocol: reverse transcription 50 °C/5 min, activation 95 °C/20 s, denaturation step 95 °C/3 s and the anneal/extension step 60 °C/30 s.

2.8. Ultrasonic-based filter-aided sample preparation

Protein digestion was performed using the Ultrasonic-based Filter-Aided Sample Preparation method (US-FASP) as described in [20]. The method combines protein alkylation with 100 µL of IAA 50 mM in 8 M Urea/ 25 mM AmBic, and trypsin digestion (1:30 trypsin-protein ratio). After proteome digestion, peptides were recovered by centrifugation. Finally, peptides were dried and stored at −20 °C until further analysis.

2.9. Analysis via MALDI-TOF-MS

Before analysis, samples were resuspended in 10 µL of formic acid 0.3 %, and 1 µL of sample was hand-spotted onto a MALDI-TOF-MS target plate and allowed to air dry. Then 1 µL of a 7 mg/mL solution of a-cyano-4-hydroxycinnamic acid matrix in 0.1 % (v/v) TFA and 50 % (v/v) ACN was added and allowed to air dry. The spectra were obtained in the positive linear mode, over a mass/charge (m/z) ratio of 600–3500, and the accelerating voltage was 20 kV. A total of 500 spectra were acquired for each sample.

2.10. Analysis via nanoLC-ESI-Q-TOF-MS/MS

The analysis was carried out using an Ultimate 3000 nano-LC system coupled to an Impact HD (Bruker Daltonics) with a CaptiveSpray nanoBooster using acetonitrile as dopant, as described previously [20]. Peptides were resuspended in 50 µL of 3 % (v/v) acetonitrile containing 0.1 % (v/v) aqueous formic acid (FA). Then, samples were homogenised for 5 min on vortex followed by 10 min on an ultrasonic bath at 100 % UA, 35 kHz ultrasonic frequency. Then, 2 µL containing 200 ng of peptides were loaded onto a trap column (µPAC™ Trapping column from PharmaFluidics) and desalted for 5 min from 3 % to 5 % B (B: 90 % acetonitrile 0.08 % FA) at a flow rate of 15 $\mu L.min^{-1}$. Then the peptides were separated using an analytical column (50 cm µPACTM PharmaFluidics) with a linear gradient at 500 $nL.min^{-1}$ (mobile phase A: aqueous FA 0.1 % (v/v); mobile phase B 90 % (v/v) acetonitrile and 0.08 % (v/v) FA) 5–90 min from 5 % to 35 % of mobile phase B, 90–100 min linear gradient from 35 % to 95 % of mobile phase B, 100–110 95 % B. Chromatographic separation was carried out at 35 °C. MS acquisition was set to cycles of MS (2 Hz), followed by MS/MS (8–32 Hz), cycle time 3.0 s, with active exclusion (precursors were excluded from precursor selection for 0.5 min after the acquisition of one MS/MS spectrum, intensity threshold for fragmentation of 2500 counts). Together with active exclusion set to 1, reconsider precursor if the intensity of a precursor increases by a factor of 3, this mass was taken from temporary exclusion list and fragmented again, ensuring that fragment spectra were taken near the peak maximum. All spectra were acquired in the

range 150–2200 *m/z*.

3. Results and discussion

3.1. Sample specimens and sample preparation

Since the onset of the disease in late 2019, different biopsies have been considered to detect and identify SARS-CoV-2 and its variants. Thus, sputum, saliva, urine, stool and nasopharynx and throat swabs have been the samples of choice for viral detection. These samples can also be used to isolate and identify other types of viruses. Currently, the upper respiratory tract is the sampling point most widely used for SARS-CoV-2, with the sample presenting one of the highest copies per specimen of standardised volume, between 10^5 to 10^9 virions [15,16,21]. The sampling is made with a swab. This approach offers several advantages, such as (i) fast sampling, typically less than 2 min; (ii) high analysis throughput via automation and (iii) it can be adapted to point-of-care devices. In addition, the swab brings not only the virus but also mucus and cells containing invaluable information about the patient's health status.

Once the sample is taken, the swab is introduced in VTM for preservation. The VTM used for sample preservation may interfere in some mass spectrometry applications as the medium contain proteins such as bovine serum albumin, and thus this fact must be taken into consideration when planning the analyses. The sample is then further processed accordingly to the downstream analysis method. Specifically for proteomics analysis, the samples are heat-inactivated for 10 min at 95 °C.

3.2. Sample handling for Immuno-mass spectrometric assay

Virus detection by mass spectrometry often requires a preconcentration step because, unlike mRNA in PCR, proteins cannot be directly amplified. Thus, the detection of minute amounts of proteins challenges MS analysis. This challenge is overcome with preconcentration techniques such as immunoaffinity, which purifies the virus whilst removing other interferences such as host- and VTM proteins. There are some methods to use immunoaffinity to extract proteins. The method we suggest yields high purity of protein and a higher recovery yield [22]. This protocol takes advantage of the information available about the virus under assessment. For instance, the S protein is known as a key protein for SARS CoV-2 infection. Therefore, the main idea consists in isolating the virion by first attaching the corresponding S antibody to the S protein to form a S protein-antibody complex. Then, magnetic particles with another protein with high affinity towards the S protein-antibody complex are added, and thus the virions get attached to these magnetic beads. Now, the magnetic beads can be separated for further sample processing, as it is explained in detail in Fig. 1 A. This method yields high-purity samples as the magnetic beads with the virus attached are isolated free of contaminants from the solution. The procedure we recommend uses 400 µL of heat-inactivated swab extract followed by the addition of 5 µL of 100 µg/mL Human monoclonal anti-SARS-CoV-2 S (S1) antibody. The mixture is then incubated for 20 min at 37 °C with gentle agitation. The length of the incubation period depends on the amount of protein material and affinity properties of the antibody; therefore, these parameters might require optimisation. Afterwards, to the virus-antibody conjugate, we add 70 µL of Protein-A Magnetic Beads (Abcam part number ab214286) followed by 20 min incubation at RT with gentle agitation. Before use, Protein A Magnetic Beads must be extensively washed with PBS to remove sodium azide, as this chemical may interfere with the conjugation of antibodies. At this stage, the supernatant can be discharged, whilst the immunoaffinity particles are recovered by placing the sample in a magnetic separator to facilitate supernatant withdrawal. Finally, magnetic beads are washed with 1 mL of phosphate-buffered saline, PBS, five times to remove non-specific binding substances. Now the virus is released by dissociating the protein-A- protein-antibody complex link. This step is done first using

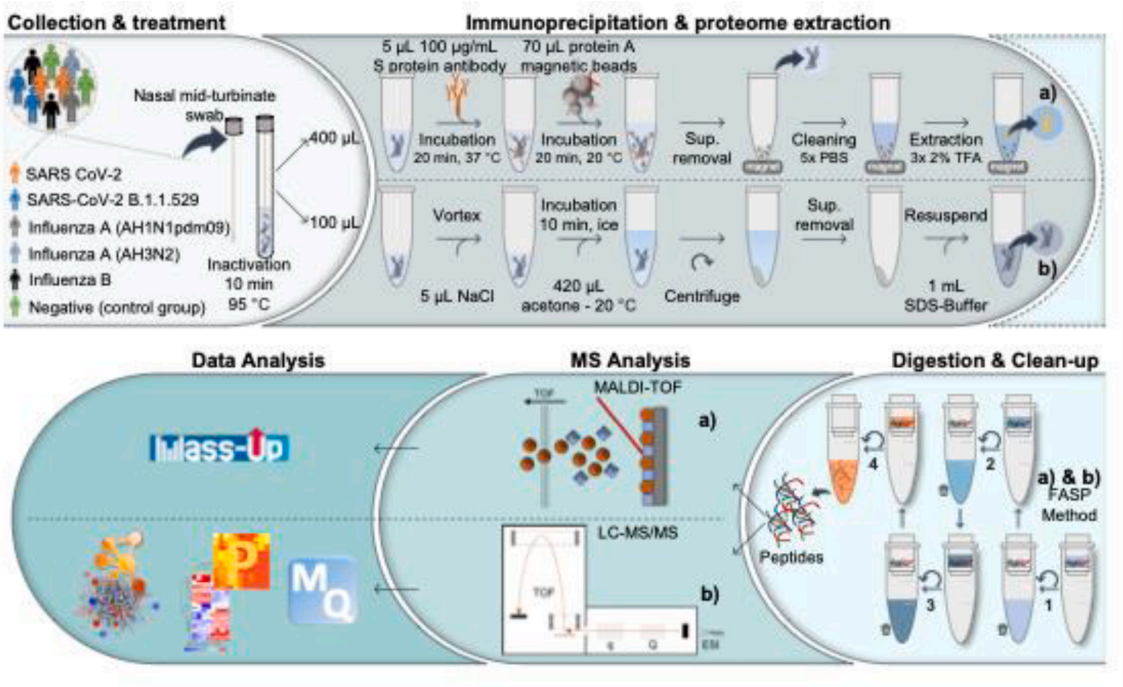

Fig. 1. Proteomics analysis workflow: from sample to analysis. (1) Sample collection & treatment. (2) Virus separation & proteome extraction a) immunoaffinity extracted proteome; b) non immunoaffinity extracted proteome. (3) Digestion & Clean-up. Ultrasonic-based Filter-Aided Sample Preparation was used for digestion and sample clean-up. (4) Mass Spectrometry analysis. Samples were analysed by MALDI-TOF-MS-TOF-MS and Nano-LC-M/MS. (5) Data analysis. Fast virus detection was achieved by MALDI-TOF-MS. analysis using the software program Mass-Up [22]. Furthermore, data processing from nanoLC-ESI-Q-TOF-MS/MS analysis was carried out in MaxQuant v(1.6.10.43) [31,32], followed by data analysis using Perseus v1.6.15 software [33]. Pathway and biochemical data interpretation were performed with the aid of the software platform Cytoscape v3.8.2 using the stringApp v1.6.0.

100 μL of 0.2 % (v/v) trifluoroacetic acid, TFA, with gentle agitation (5 min). The supernatant is withdrawn using a magnetic separator, and then the process is repeated. The volumes extracted are pooled together. Finally, 200 μL of 4 % (w/v) Sodium dodecyl sulphate, SDS, in Tris-HCl pH 8.5, 50 mM 1,4-Dithio-DL-threitol, DTT, is added to the magnetic beads. This solution is the standard one to use in the FASP protocol, and it is now withdrawn using a magnetic separator. The TFA and SDS extracts containing the virions are combined and subjected to ultrasonic-based filter-assisted sample preparation, US-FASP, as described by Carvalho et al. [20]. In brief, the TFA-SDS extract is loaded in a Vivacon 500 10.000 molecular weight cut-off, MWCO, and centrifuged for 20 min at 14 000g. High molecular weight molecules (>10 kDa) are retained on top of the ultrafiltration membrane, whereas low molecular weight contaminants are filtered through the membrane. To remove SDS, the proteins in the membrane are then washed with 200 μL of 8 M urea and 25 mM AmBic solution (centrifuged for 20 min at 14 000g). Protein alkylation is performed in the ultrafiltration membrane. First, by adding 100 μL of 50 mM iodoacetamide (IAA) in 8 M urea and 25 mM AmBic solution. The alkylation step was sped up using the ultrasonic microplate horn assembly for 5.25 min (7 cycles: 30 s on and 15 s off UT, 25 % ultrasonic amplitude, UA, 20 kHz ultrasonic frequency, UF). Subsequently, IAA solution is removed by centrifugation. Before performing trypsin digestion, the samples must be washed with an appropriate buffer to remove urea because this reagent is a strong chaotropic agent which hampers enzymatic digestion. Thus, the sample is washed twice with 200 μL of 25 mM AmBic. Finally, 100 μL of 1:30 trypsin in 12.5 mM, Ammonium bicarbonate, AmBic solution was added, and the protein digestion was processed using the ultrasonic microplate horn assembly for 5.25 min (7 cycles: 30 s on and 15 s off UT, 25 % UA, 20 kHz UF) [19]. Then the peptides are collected after 20 min of centrifugation at 14 000g. To ensure that all the peptides were extracted, 100 μL of 3 % (v/v) acetonitrile and 0.1 % (v/v) formic acid were added, followed by centrifugation of 20 min at 14 000g. This step was repeated one more time, and then extracts containing the peptides were transferred to a 500 μL microtube, dried, and stored at − 20 °C until further analysis by MALDI-TOF-MS or by Nano-LC-MS/MS.

To show that the virus separation approach works, we used electron microscopy, EM, to visualise the virus attached to the magnetic beads. In addition, RT-PCR was used to confirm the presence of SARS-CoV-2 RNA. Fig. 2A-D shows EM photographs where the virion is observed linked to the magnetic beads, whereas Fig. 2E-F shows EM photographs with cells infected with the virus. The same samples tested positive for SARS-CoV-2 (RT-PCR), as shown in Fig. 2 left table. Furthermore, to verify the range of applicability of this approach, we assayed the virus separation method with solutions containing different virus loads ranging from 20 to 2000 viral particles. The different virus loads present in each sample are reflected by the different number of cycles needed to confirm the presence of the virus via RT-PCR (see table in Fig. 2). As expected, the lower the virus load, the higher the number of RT-PCR cycles needed for detection.

3.3. Sample handling for medical proteomic analysis

The entire proteome obtained using a swab contains information about the patient's response to the infection, and so it must be kept in mind that further information is retrieved from the sample. The handling here suggested to treat this sample is the classic proteome precipitation based on acetone incubation on ice, followed by centrifugation and resuspension as described in Fig. 1b. To this end, an amount of 100 μL from the swab extract is mixed with NaCl to a final concentration of 10 mM and then incubated with acetone at −20 °C. This simple procedure promotes the precipitation of all proteins in solution. Finally, the supernatant is removed, and the precipitate is resuspended in 400 μL SDS buffer (2 % (w/v) SDS in Tris-HCl pH 8.5, 50 mM DTT) using an ultrasonic probe UP100 (50 % ultrasonic amplitude, 10 s ultrasonication time), and the total protein content is determined by Bradford protein assay. Then 50 μg of total protein is digested using the US-FASP procedure as described in section 3.2. This sample is used to get proteomics insights into the host-virus cross-talk.

3.4. Fast virus detection via MALDI-TOF-MS analysis

Although different laboratories have their own biases associated with the MALDI-TOF-MS configurations at hand, it is worth noting that the MALDI-TOF-MS used in this work, was selected because it is the standard one nowadays available in most hospitals where it is regularly used for bacterial identification [22].

We recommend working on the information rendered by the MALDI-TOF-MS spectra using an in-house made program developed by our team called Mass-Up [23]. This program is friendly to use, and there is an online tutorial available [23]. Furthermore, it allows to perform (i) clustering, (ii) principal component analysis and (iii) to identify unique peptide masses for each sample.

Gibb et al. also have contributed to the community with the open-source MALDIquant software [24]. MALDI-TOF-MS was one of the first mass spectrometry tools reported to detect SARS-CoV-2 [24]. However, early studies focused on the MALDI-TOF-MS analysis of nasopharyngeal swab solutions were made using the total proteome

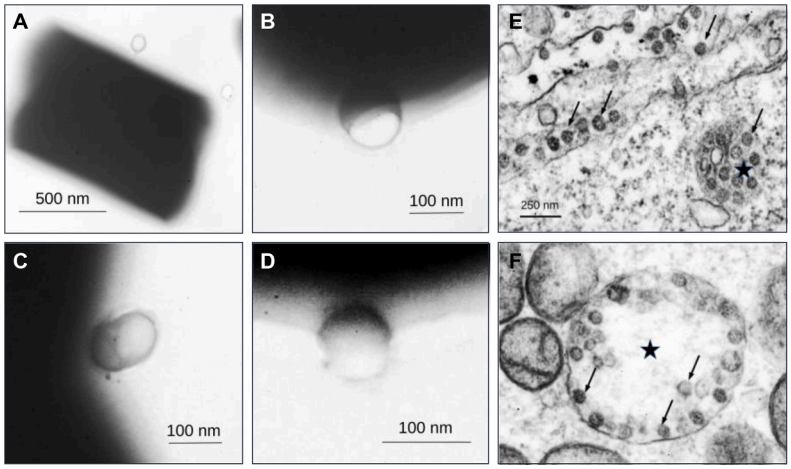

Gene	PFUs	CTs
ORF1ab	20	32±2
ORF1ab	200	28±2
ORF1ab	2000	25±1
ORF1ab	POS-CTRL	16±1
ORF1ab	NEG-CTRL	n.d.
E	20	29±2
E	200	26±1
E	2000	23±1
E	POS-CTRL	18±1
E	NEG-CTRL	n.d.
N	20	28±1
N	200	24±1
N	2000	22±1
N	POS-CTRL	28±1
N	NEG-CTRL	n.d.

Fig. 2. TEM images of the SRAS-CoV-2 immunoaffinity extracts and the Cycle thresholds (CTs) obtained by RT-PCR. A – D. Magnetic beads with attached vesicle-like particles. Spikes do not show, probably due to loss during specimen preparation. E – F. Extracellular COVID particles (E - arrows) and cytoplasmic vacuoles filled with COVID particles (F - arrows) replicating in Vero cells used for virus production.

extracted with the swab, i.e. the virus plus the host proteomes. As could be expected, the components present in the sample other than the virus made MALDI-TOF-MS interpretation difficult. Thus, a high degree of variability among samples is expected. This was the case when a total of 362 specimens (comprising 211 positive and 151 negative samples) from three different laboratories were subjected to MALDI-TOF-MS analysis [24]. Thus, this study only rendered the *m/z* peak 7612 common to all spectra across all laboratories, and only *m/z* peak at 3358 to differentiate the control group from SARS-CoV-2 group. This data suggests that a larger number of samples could possibly not be distinguishable. Furthermore, problems to identify/classify the virus are anticipated due to virus mutations. Further uses of MALDI-TOF-MS in this line of research provide a positive predictive value of 60 % and a negative predictive value of 73.2 % in a study conducted with 311 patients [25].

To exemplify the problems derived from using the whole swab sample with no sample treatment, we compared it with the virus separation procedure by MALDI-TOF-MS. We included viruses from two SARS-CoV-2 variants, the three influenza types/subtypes causing seasonal epidemics, and a control group. Data interpretation using the Mass-UP program showed that influenza and SARS-CoV-2 viruses could not be differentiated when the whole swab sample was used. This result is easily explained due to the presence of molecules originating in the host's cells and the bovine proteins used for sample preservation in the swab extracts. The *m/z* signal of such molecules dominates the MALDI-TOF-MS spectra, hampering classification because they mask and suppress the ionisation of viral proteins as they are at lower concentrations. On the other hand, the virus separation process promotes virus enrichment and sample clean-up, substantially improving the detection of viral peptide signals and improving MALDI-TOF-MS shot-to-shot and sample-

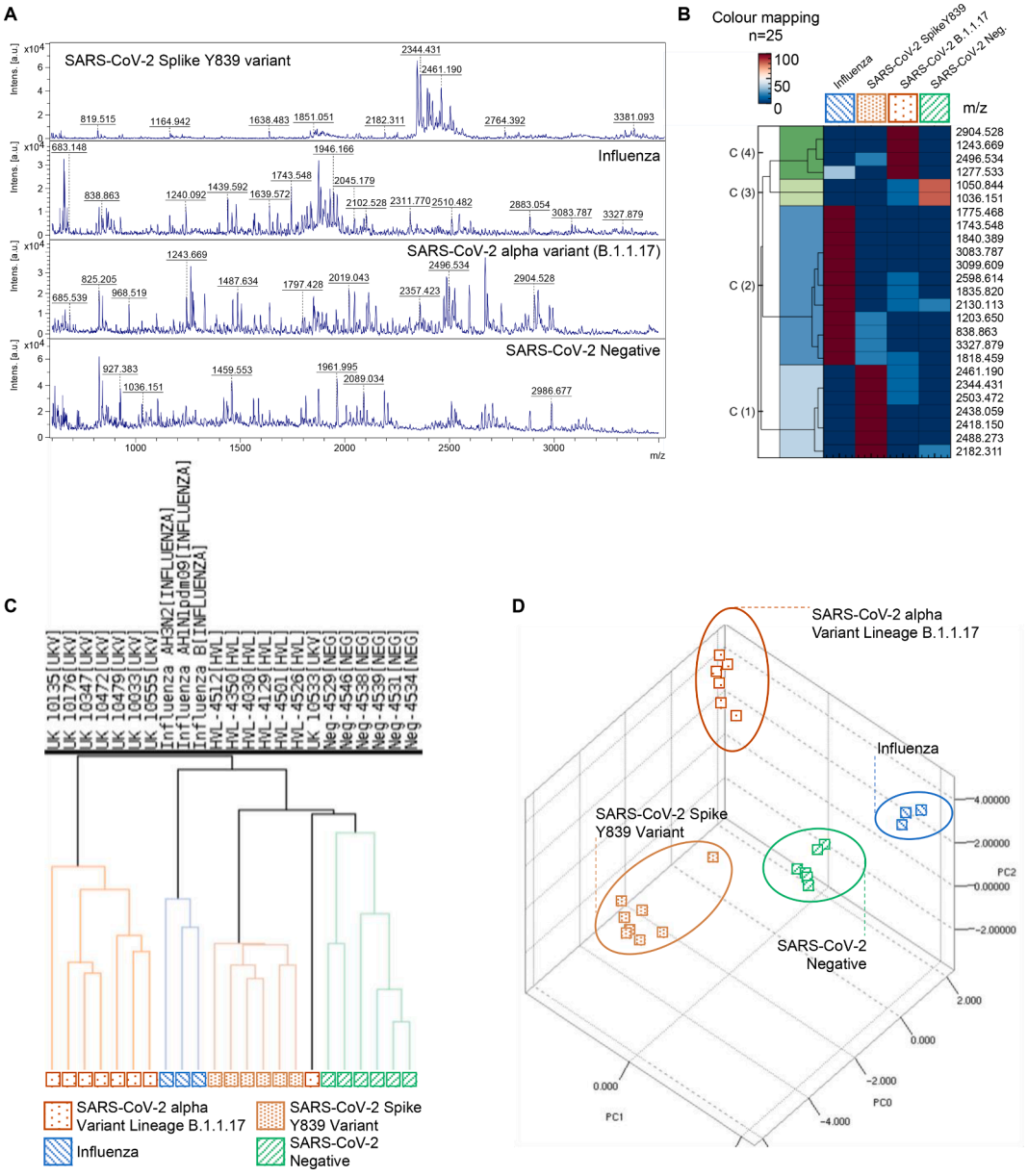

Fig. 3. MALDI-TOF-MS SARS-CoV-2 detection. A. Representative MALDI-TOF-MS spectra of SARS-CoV-2 Spike Y839, Influenza B, SARS-CoV-2 alpha variant (B.1.1.17) and SARS-CoV-2 Negative. B. Colour mapping of the representative *m/z* signals. The colour scale represents the percentage of presence in the MALDI-TOF-MS spectra (0 not present, 100% present in all spectra); C1 discriminant *m/z* signals for SARS-CoV-2 Spike Y839, *C2* is C1 discriminant *m/z* signals for Influenza B, C3 discriminant *m/z* signals for SARS-CoV-2 negative and C4 discriminant *m/z* signals for SARS-CoV-2 alpha variant (B.1.1.17). C. Hierarchical cluster generated with the discriminant *m/z* signals. D. Principal component analysis generated with the discriminant *m/z* signals.

to-sample reproducibility. Representative MALDI-TOF-MS spectra are shown in Fig. 3A.

Moreover, the Mass-UP program delivered a list of unique *m/z* peaks that allowed for the rapid detection of SARS-CoV-2. For instance, the SARS-CoV-2 Spike Y839 variant can be identified with *m/z* signals 2182.31, 2418.15, 2438.06, 2488.27, 2344.43, 2461.19, 2503.47, whereas the Alpha variant (B.1.1.7 lineage) can be identified with the *m/z* peaks 1243.67, 1277.53, 2904.53 and 2496.53. Fig. 3B shows the classification of the samples done via cluster using the unique peptides found using the MASS up program, where it is worth noting that multiple enzymatic digestions would render an extended list of *m/z* peptide signals. All viruses are differentiated and grouped via clustering, as shown in Fig. 3C. Further confirmation of the consistency of the clustering classification was obtained via Principal Component Analysis, as the samples were also grouped by class (Fig. 3D). Furthermore, and when possible, the use of MALDI-TOF-MS/MS would add an extra dimension of analysis due to peptide sequencing capabilities, making it possible to differentiate virus variants at the peptide sequence level. Some authors have also suggested the possibility of analysing the intact virus proteins without enzymatic digestion [17]. Still, this method would render fewer *m/z* peaks than a collection of peptides from a digested sample. Also, due to the low resolution of the MALDI-TOF-MS used, the identification of *m/z* signals for the Spike protein would not allow for the distinction of SARS-CoV-2 variants unless many mutations are present.

3.5. Virus detection via nanoLC-ESI-Q-TOF-MS/MS analysis

The use of nanoLC-ESI-Q-TOF-MS/MS in the strategy of fighting virus pandemics presents several advantages but also several drawbacks when compared to MALDI-TOF-MS. High resolution nanoLC-ESI-Q-TOF-MS/MS is nowadays a popular instrument in many research laboratories and facilities, yet it is uncommon in most hospitals. Also, the analysis done via ESI takes much time, from some tens of minutes to hours, if compared with MALDI-TOF-MS, where taking a single spectrum via a laser shot typically takes seconds. On the other hand, more information is retrieved with ESI than via MALDI-TOF-MS that can be used for the patient's benefit via prognosis using proteomic analysis, as we will show in the next section. Again, literature provides clues about when and how ESI must be used. For instance, the strategy of using the whole host proteome as derived from the swab with no cleaning and preconcentrating strategies has been shown ineffective, as few viral peptides are identified. For instance, of nine positive clinical samples, only viral peptides were detected in two of them [26]. Approaches using reaction monitoring strategies present a short analysis time, of the order of some minutes, being able to detect up to 84 % of the positive cases confirmed by RT-PCR with up to 97 % specificity (985 samples) [27]. Yet they present time-consuming treatment protocols that cannot be circumvented, rendering an inefficient tool for fast high throughput screening analysis if compared with MALDI-TOF-MS [11]. Although complex in its design, it is also worth mentioning the work developed by Cardozo et al., who claim to analyse 4 samples every 10 min using parallel reaction monitoring with a 97 % specificity and 84 % of selectivity [27].

3.6. Proteomic analysis via nanoLC-ESI-Q-TOF-MS/MS analysis

The utility of ESI in the context of a pandemic is to analyse the patient's proteome and to render information about the dysregulation of biochemical pathways involved in the host's defence. In other words, to answer if the response caused by the virus is getting decontrolled with consequences for the patient going from the need to intensive care to dead. To exemplify this application, we compare the proteomes obtained from swabs of nasopharyngeal and oropharyngeal negative patients against patients infected with SARS-CoV-2 Spike Y839 and SARS-CoV-2 Alpha (B.1.1.7) variants and influenza B and AH1N1pdm09 and AH3N2 viruses, as shown in Fig. 4A. A total of 437 proteins were quantified in this work (Supplementary information SI1). Differential expression analysis is shown in Fig. 4B as volcano plots. The relative quantification data shows that that the number of proteins differentially expressed is higher in patients with SARS-CoV-2 Spike Y839 and SARS-CoV-2 Alpha (B.1.1.7) variants, suggesting a higher dysregulation of the biochemical pathways linked to disease response. As shown in Fig. 4C, when the dysregulated proteins obtained for each volcano plot are used to compare patients via protein–protein interaction pathway, eight pathways linked with the immune system arise significantly dysregulated. As it can be seen, the SARS-CoV-2-infected patients are grouped, showing a response largely dysregulated when compared with the influenza-infected patients for the following biochemical pathways: (*P*1) blood coagulation; (*P*2) platelet aggregation; (*P*3) leukocyte activation; (*P*4) processing & presentation of exogenous peptide antigen via MHC; (P5) antimicrobial humoral response; (*P*6) leukocyte mediated immunity; (P7) the neutrophil degranulation and (P8) innate immune system. The largest dysregulation was presented by the SARS-CoV-2 Alpha (B.1.1.7) variant, having the largest dysregulation for pathways *P*6, P7 and P8. As it may be seen, the amount of information retrieved from this approach is enormous. Just to mention some examples, Fig. 4D shows selected proteins at different levels of dysregulation in SARS-CoV-2 Spike Y839 variant and SARS-CoV-2 Alpha (B.1.1.7)-infected patients. As a first example, protein C4B activates the complement system via the lectin pathway, one of the first pathways activated to defend organisms when there are no specific antibodies against antigens. When this pathway is out of control, however, reactions leading to unnecessary inflammation and death of healthy cells occur [28,29]. This protein was found overexpressed in the SARS-CoV-2 Alpha (B.1.1.7) variant, precisely the most aggressive of the viruses used in this study (Log2 transformed LFQ values for (a) SARS-CoV-2 Alpha (B.1.1.7) variant 17.4 $\pm$ 1.5, n = 8; (b) SARS-CoV-2 Spike Y839 variant 14.6 $\pm$ 1.3, n = 6 and (c) SARS-CoV-2 negative 14.7 $\pm$ 1.8, n = 6). As the second example, the Bactericidal/permeability-increasing fold containing family A, member 1 (BPIFA1), is a secretory protein found in human upper aerodigestive tract mucosa. This innate material is secreted in mucosal fluid or found in submucosal tissue in the human soft palate, lung, uvula, and nasal cavity [30]. BPIFA1 is a critical component of the innate immune response that prevents upper airway diseases, and it was found upregulated in SARS-CoV-2 Alpha (B.1.1.7) variant (Log2 transformed LFQ values for (a) SARS-CoV-2 Alpha (B.1.1.7) variant 20.5 $\pm$ 1.8, n = 8; (b) SARS-CoV-2 Spike Y839 variant 16.5 $\pm$ 1.8, n = 6 and (c) SARS-CoV-2 negative 13.9 $\pm$ 1.5, n = 6). The overexpression of both proteins describes a clinical process where the SARS-CoV-2 Alpha (B1.1.7)-infected patients are responding in a more aggressive manner than the SARS-CoV-2 Spike Y839 variant-infected patients.

4. Conclusions

Future pandemics will be defeated at the analytical chemistry laboratory. The low limit of detection, robustness, high mass accuracy and resolution of modern mass spectrometry combined with high separation capacity of microseparation techniques and appropriate sample pretreatments will lead to an unprecedented level of sample handling and information delivery. Immunoextraction using magnetic beads seems to be called a very suitable sample treatment to study viruses and virus infections by MS. Also, medical analytical chemistry derived from the proteomics ability to interpret the host answer to the virus infection will play an important role in assessing prognosis and even prescriptions for

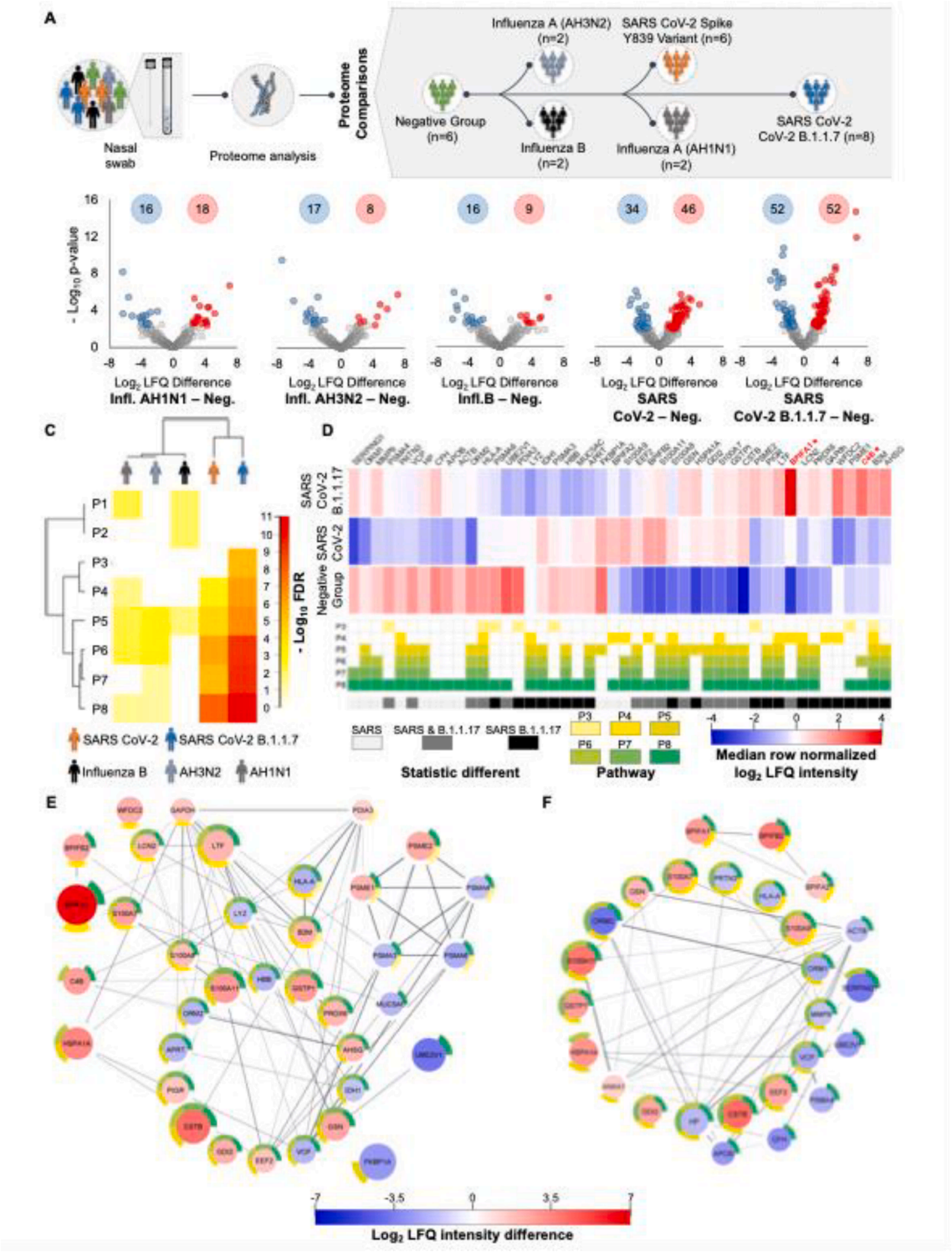

(caption on next page)

patients. Thus, Analytical Chemistry and MALDI-TOF-MS/MS are called to play an important role in virus identification, whereas Analytical Chemistry and nanoLC-ESI-Q-TOF-MS/MS mass spectrometry will play it at the medical level via analytical proteomics and bioinformatics.

Declaration of Competing Interest

The authors declare that they have no known competing financial interests or personal relationships that could have appeared to influence the work reported in this paper.

Fig. 4. Proteome and protein–protein network analysis of SARS CoV-2 (Spike Y839 variant) and Alpha Variant SARS-CoV-2B.1.1.7 patients. A. Workflow used for proteome comparisons. Protein levels of patients with SARS CoV-2 Spike Y839, SARS-CoV-2B.1.1.7, Influenza B, Influenza A (AH3N2) and Influenza A (AH1N1) were compared against a negative control group of patients. B. Volcano plot showing the differently expressed proteins on the different groups of patients compared. Circles represent proteins in which the colour represents grey: non-statistic proteins, blue: downregulated proteins and red: up-regulated proteins. A student's *t*-test (FDR 0.05 and S0 of 0.1) was used for statistical analysis. C. Cluster analysis of the related immune response pathways. In each group, FDR values for each pathway related to immune response were selected and analysed on a hierarchical cluster (average linkage, no constraint, pre-processing with k-means, and Euclidean distance). *P*1 - Blood coagulation; *P*2 - Platelet aggregation; *P*3 - Leukocyte activation; *P*4 - Antigen processing and presentation of exogenous peptide antigen via MHC class I, TAP-dependent; P5 - Antimicrobial humoral response; *P*6 - Leukocyte mediated immunity; P7 - Neutrophil degranulation; P8 - Innate Immune System. D. Heatmap showing the expression levels of the differential proteins enrolled in the immune response-related pathways. Pathway colour gradient represents the following pathways: *P*3 - Leukocyte activation; *P*4 - Antigen processing and presentation of exogenous peptide antigen via MHC class I, TAP-dependent; P5 - Antimicrobial humoral response; *P*6 - Leukocyte mediated immunity; P7 - Neutrophil degranulation; P8 - Innate Immune System. Black coloured squares represent the differential proteins found in the SARS-CoV-2B.1.1.7 patients. Grey-coloured squares represent the differential proteins found in the SARS CoV-2 Spike Y839 variant and SARS-CoV-2B.1.1.7 patients. White-grey coloured squares represent the differential proteins found in the SARS CoV-2 Spike Y839 variant patients. E. SARS-CoV-2B.1.1.7 protein–protein interaction pathway analysis. F. SARS CoV-2 **Spike Y839 variant** protein–protein interaction analysis. Protein-protein interaction was performed in the software platform Cytoscape v3.8.2 [34] using the stringApp v1.6.0. [35] Briefly, the statistically significant proteins were imported to a network using the string protein query data source. Furthermore, functional analysis was performed using a STRING enrichment. Reactome and Kyoto Encyclopedia of Genes and Genomes (KEGG) were used as pathway databases. (For interpretation of the references to colour in this figure legend, the reader is referred to the web version of this article.)

Data availability

Data will be made available on request.

Acknowledgements

PROTEOMASS Scientific Society is acknowledged by the funding provided to the Laboratory for Biological Mass Spectrometry Isabel Moura (#PM001/2019 and #PM003/2016). H.M.S, L.B.C. C.L., G.M., and J.L.C. acknowledge the funding provided by the Associate Laboratory for Green Chemistry LAQV which is financed by national funds from FCT/MCTES, *Fundação para a Ciência e Tecnologia*and *Ministério da Ciência, Tecnologia e Ensino Superior*, through the projects UIDB/50006/2020 and UIDP/50006/2020. H.M.S acknowledges the Associate Laboratory for Green Chemistry-LAQV (LA/P/0008/2020) funded by FCT/MCTES for his research contract. L.B.C., G.M. thank FCT/MCTES (Portugal) for their PhD grant (SFRH/BD/144222/2019) and (SFRH/BD/139384/2018), respectively. The authors acknowledge Dr. Miguel Fevereiro from INIAV for his valuable help and fruitful discussions.

Funding

This work received financial support from PT national funds (FCT/MCTES) through the projects UIDB/50006/2020 and UIDP/50006/2020 and from PROTEOMASS Scientific Society through the projects #PM001/2019 and #PM003/2016.

Appendix A. Supplementary data

Supplementary data to this article can be found online at https://doi.org/10.1016/j.microc.2022.108323.

References

[1] https://covid19.who.int. Last time accessed July 4th 2022.
[2] F. Wu, S. Zhao, B. Yu, Y.M. Chen, W. Wang, Z.G. Song, Y. Hu, Z.W. Tao, J.H. Tian, Y.Y. Pei, M.L. Yuan, Y.L. Zhang, F.H. Dai, Y. Liu, Q.M. Wang, J.J. Zheng, L. Xu, E. C. Holmes, Y.Z. Zhang, A new coronavirus associated with human respiratory disease in China, Nature. 579 (2020) 265–269, https://doi.org/10.1038/s41586-020-2008-3.
[3] P. Zhou, X. Lou Yang, X.G. Wang, B. Hu, L. Zhang, W. Zhang, H.R. Si, Y. Zhu, B. Li, C.L. Huang, H.D. Chen, J. Chen, Y. Luo, H. Guo, R. Di Jiang, M.Q. Liu, Y. Chen, X. R. Shen, X. Wang, X.S. Zheng, K. Zhao, Q.J. Chen, F. Deng, L.L. Liu, B. Yan, F. X. Zhan, Y.Y. Wang, G.F. Xiao, Z.L. Shi, A pneumonia outbreak associated with a new coronavirus of probable bat origin, Nature. 579 (2020) 270–273, https://doi.org/10.1038/s41586-020-2012-7.
[4] N. Zhu, D. Zhang, W. Wang, X. Li, B. Yang, J. Song, X. Zhao, B. Huang, W. Shi, R. Lu, P. Niu, F. Zhan, X. Ma, D. Wang, W. Xu, G. Wu, G.F. Gao, W. Tan, A Novel Coronavirus from Patients with Pneumonia in China, N. Engl. J. Med. 382 (2020) (2019) 727–733, https://doi.org/10.1056/NEJMOA2001017.
[5] Z. Wu, J.M. McGoogan, Characteristics of and important lessons grom the coronavirus disease 2019 (COVID-19) outbreak in China: Summary of a report of 72 314 cases from the Chinese Center for Disease Control and Prevention, JAMA. 323 (2020) 1239–1242. doi:10.1001/JAMA.2020.2648.
[6] J. Hedman, P. Rådström, Overcoming Inhibition in Real-Time Diagnostic PCR, In: Wilks, M. (eds) PCR Detection of Microbial Pathogens. Methods in Molecular Biology, vol 943. Humana Press, Totowa, NJ. doi: 10.1007/978-1-60327-353-4_2.
[7] Y. Pan, L. Long, D. Zhang, T. Yuan, S. Cui, P. Yang, Q. Wang, S. Ren, Potential false-negative nucleic acid testing results for severe acute respiratory syndrome coronavirus 2 from thermal inactivation of samples with low viral loads, Clin. Chem. 66 (2020) 794–801, https://doi.org/10.1093/CLINCHEM/HVAA091.
[8] S.A. Trauger, T. Junker, G. Siuzdak, Investigating viral proteins and intact viruses with mass spectrometry, in: Mod. Mass Spectrom., Springer, Berlin, Heidelberg, 2003: pp. 265–282. doi:10.1007/3-540-36113-8_8.
[9] K.M. Downard, B. Morrissey, A.B. Schwahn, Mass spectrometry analysis of the influenza virus, Mass Spectrom. Rev. 28 (2009) 35–49, https://doi.org/10.1002/MAS.20194.
[10] L.M. Ganova-Raeva, Y.E. Khudyakov, Application of mass spectrometry to molecular diagnostics of viral infections, Expert Rev. Mol. Diagn. 13 (2014) 377–388, https://doi.org/10.1586/ERM.13.24.
[11] A. Milewska, J. Ner-Kluza, A. Dabrowska, A. Bodzon-Kulakowska, K. Pyrc, P. Suder, Mass spectrometry in virological sciences, Mass Spectrom. Rev. 39 (2020) 499–522, https://doi.org/10.1002/MAS.21617.
[12] P. Singh, R. Chakraborty, R. Marwal, V S Radhakrishan, Akash, K. Bhaskar, H. Vashisht, M.S. Dhar, S. Pradhan, G. Ranjan, M. Imran, A. Raj, U. Sharma, P. Singh, H. Lall, Meena Dutta, P. Garg, A. Ray, Debasis Dash, Sridhar Sivasubbu, H. Gogia, Preeti Madan, S. Kabra, Sujeet, K. Singh, A. Agrawal, P. Rakshit, Pramod Kumar, S. Sengupta, A rapid and sensitive method to detect SARS-CoV-2 virus using targeted-mass spectrometry, J. Proteins Proteomics 2020. 11 (2020) 159–165. doi:10.1007/S42485-020-00044-9.
[13] X. He, E.H.Y. Lau, P. Wu, X. Deng, J. Wang, X. Hao, Y.C. Lau, J.Y. Wong, Y. Guan, X. Tan, X. Mo, Y. Chen, B. Liao, W. Chen, F. Hu, Q. Zhang, M. Zhong, Y. Wu, L. Zhao, F. Zhang, B.J. Cowling, F. Li, G.M. Leung, Temporal dynamics in viral shedding and transmissibility of COVID-19, Nat. Med. 26 (2020) 672–675, https://doi.org/10.1038/s41591-020-0869-5.
[14] K.K.W. To, O.T.Y. Tsang, W.S. Leung, A.R. Tam, T.C. Wu, D.C. Lung, C.C.Y. Yip, J. P. Cai, J.M.C. Chan, T.S.H. Chik, D.P.L. Lau, C.Y.C. Choi, L.L. Chen, W.M. Chan, K. H. Chan, J.D. Ip, A.C.K. Ng, R.W.S. Poon, C.T. Luo, V.C.C. Cheng, J.F.W. Chan, I.F. N. Hung, Z. Chen, H. Chen, K.Y. Yuen, Temporal profiles of viral load in posterior oropharyngeal saliva samples and serum antibody responses during infection by SARS-CoV-2: an observational cohort study, Lancet Infect. Dis. 20 (2020) 565–574, https://doi.org/10.1016/S1473-3099(20)30196-1.
[15] L. Zou, F. Ruan, M. Huang, L. Liang, H. Huang, Z. Hong, J. Yu, M. Kang, Y. Song, J. Xia, Q. Guo, T. Song, J. He, H.-L. Yen, M. Peiris, J. Wu, SARS-CoV-2 Viral Load in Upper Respiratory Specimens of Infected Patients, N. Engl. J. Med. 382 (2020) 1177–1179, https://doi.org/10.1056/NEJMc2001737.
[16] N.L. Dollman, J.H. Griffin, K.M. Downard, Detection, mapping, and proteotyping of SARS-CoV-2 coronavirus with high resolution mass spectrometry, ACS Infect. Dis. 6 (2020) 3269–3276, https://doi.org/10.1021/acsinfecdis.0c00664.
[17] R.K. Iles, R. Zmuidinaite, J.K. Iles, G. Carnell, A. Sampson, J.L. Heeney, Development of a Clinical MALDI-TOF-Mass Spectrometry Assay for SARS-CoV-2: Rational Design and Multi-Disciplinary Team Work, Diagnostics. 10 (2020) 746, https://doi.org/10.3390/DIAGNOSTICS10100746.
[18] J.H. Griffin, K.M. Downard, Mass spectrometry analytical responses to the SARS-CoV2 coronavirus in review, TrAC - Trends Anal. Chem. 142 (2021), 116328, https://doi.org/10.1016/j.trac.2021.116328.
[19] World Health Organization (WHO), Coronavirus disease (COVID-19) technical guidance: Laboratory testing for 2019-nCoV in humans. https://www.who.int/emergencies/diseases/novel-coronavirus-2019/technical-guidance/laboratory-guidance/ (Last time accessed July 4th 2022).
[20] L.B. Carvalho, J.L. Capelo-Martínez, C. Lodeiro, J.R. Wiśniewski, H.M. Santos, Ultrasonic-based filter aided sample preparation as the general method to sample preparation in proteomics, Anal. Chem. 92 (2020) 9164–9171, https://doi.org/10.1021/acs.analchem.0c01470.

[21] W. Tian, N. Zhang, R. Jin, Y. Feng, S. Wang, S. Gao, R. Gao, G. Wu, D. Tian, W. Tan, Y. Chen, G.F. Gao, C.C.L. Wong, Immune suppression in the early stage of COVID-19 disease, Nat. Commun. 11 (2020) 1–8, https://doi.org/10.1038/s41467-020-19706-9.

[22] (a) https://www.abcam.com/protocols/immunoprecipitation-protocol-1, last time accessed 23, November, 2022. (b) T. Maier, S. Klepel, U. Renner, M. Kostrzewa. Fast and reliable MALDI-TOF-MS–based microorganism identification. Nat Methods 3 (2006) i–ii. doi: 10.1038/nmeth870.

[23] H. López-Fernández, H.M. Santos, J.L. Capelo, F. Fdez-Riverola, D. Glez-Peña, M. Reboiro-Jato, Mass-Up: An all-in-one open software application for MALDI-TOF mass spectrometry knowledge discovery, BMC Bioinformatics. 16 (2015) 1–12, https://doi.org/10.1186/S12859-015-0752-4.

[24] (a) S. Gibb, K. Strimemr, Mass spectroemtry analysis using MALDIquant. In Statistical Analysis of Proteomics, Metabolomics, and Lipidomics Data Using Mass Spectrometry. Springer editors. 2016, 101-124. (b) F.M. Nachtigall, A. Pereira, O.S. Trofymchuk, L.S. Santos, Detection of SARS-CoV-2 in nasal swabs using MALDI-MS, Nat. Biotechnol. 38 (2020) 1168–1173. doi:10.1038/s41587-020-0644-7.

[25] M.F. Rocca, J.C. Zintgraff, M.E. Dattero, L.S. Santos, M. Ledesma, C. Vay, M. Prieto, E. Benedetti, M. Avaro, M. Russo, F.M. Nachtigall, E. Baumeister, A combined approach of MALDI-TOF mass spectrometry and multivariate analysis as a potential tool for the detection of SARS-CoV-2 virus in nasopharyngeal swabs, J. Virol. Methods. 286 (2020), 113991, https://doi.org/10.1016/J.JVIROMET.2020.113991.

[26] D. Gouveia, G. Miotello, F. Gallais, J.C. Gaillard, S. Debroas, L. Bellanger, J. P. Lavigne, A. Sotto, L. Grenga, O. Pible, J. Armengaud, Proteotyping SARS-CoV-2 Virus from Nasopharyngeal Swabs: A Proof-of-Concept Focused on a 3 Min Mass Spectrometry Window, J. Proteome Res. 19 (2020) 4407–4416, https://doi.org/10.1021/ACS.JPROTEOME.0C00535.

[27] K.H.M. Cardozo, A. Lebkuchen, G.G. Okai, R.A. Schuch, L.G. Viana, A.N. Olive, C. dos S. Lazari, A.M. Fraga, C.F.H. Granato, M.C.T. Pintão, V.M. Carvalho, Establishing a mass spectrometry-based system for rapid detection of SARS-CoV-2 in large clinical sample cohorts, Nat. Commun. 11 (2020) 1–13. doi:10.1038/s41467-020-19925-0.

[28] J. Dunkelberger, W.C. Song, Complement and its role in innate and adaptive immune responses, Cell Res 20 (2010) 34–50, https://doi.org/10.1038/cr.2009.139.

[29] M.M. Lamers, B.L. Haagmans, SARS-CoV-2 pathogenesis, Nat. Rev. Microbiol. 20 (2022) 270–284, https://doi.org/10.1038/s41579-022-00713-0-.

[30] C.J. Britto, L. Cohn, Bactericidal/Permeability-increasing protein fold-containing family member A1 in airway host protection and respiratory disease, Am. J. Respir. Cell Mol. Biol. 52 (5) (2015) 525–534, https://doi.org/10.1165/rcmb.2014-0297RT.

[31] J. Cox, M. Mann, MaxQuant enables high peptide identification rates, individualised p.p.b.-range mass accuracies and proteome-wide protein quantification, Nat. Biotechnol. 26 (12) (2008) 1367–1372, https://doi.org/10.1038/nbt.1511.

[32] S. Tyanova, T. Temu, J. Cox, The MaxQuant computational platform for mass spectrometry-based shotgun proteomics, Nat. Protoc. 11 (12) (2016) 2301–2319, https://doi.org/10.1038/nprot.2016.136.

[33] S. Tyanova, J. Cox, Perseus: a bioinformatics platform for integrative analysis of proteomics data in cancer research, Methods Mol. Biol. (2018) 133–148, https://doi.org/10.1007/978-1-4939-7493-1_7.

[34] P. Shannon, A. Markiel, O. Ozier, N.S. Baliga, J.T. Wang, D. Ramage, N. Amin, B. Schwikowski, T. Ideker, Cytoscape: a software environment for integrated models of biomolecular interaction networks, Genome Res. 13 (11) (2003) 2498–2504, https://doi.org/10.1101/gr.1239303.

[35] N.T. Doncheva, J.H. Morris, J. Gorodkin, L.J. Jensen, Cytoscape StringApp: Network Analysis and Visualization of Proteomics Data, J. Proteome Res. 18 (2) (2019) 623–632, https://doi.org/10.1021/acs.jproteome.8b00702.